Accepted Manuscript

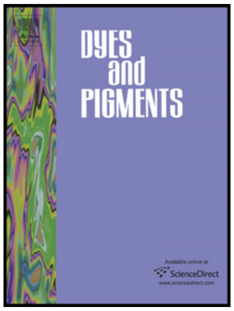

Novel Cyclometalated Platinum (II) Complex Containing Carrier- Transporting Groups: Synthesis, Luminescence and Application in Single-dopant White PLEDs

Aihui Liang, Yanhu Li, Weiguo Zhu, Yafei Wang, Fei Huang, Hongbin Wu, Yong Cao

PII: S0143-7208(12)00306-3
DOI: 10.1016/j.dyepig.2012.11.006
Reference: DYPI 3765

To appear in: *Dyes and Pigments*

Received Date: 29 August 2012
Revised Date: 4 November 2012
Accepted Date: 6 November 2012

Please cite this article as: Liang A, Li Y, Zhu W, Wang Y, Huang F, Wu H, Cao Y, Novel Cyclometalated Platinum (II) Complex Containing Carrier- Transporting Groups: Synthesis, Luminescence and Application in Single-dopant White PLEDs, *Dyes and Pigments* (2012), doi: 10.1016/j.dyepig.2012.11.006.

Highlights

1. Two novel platinum complexes derived from 2(2,4-difluorophenyl)pyridine were synthesized.

2. The photophysical and electroluminescent properties of the platinum complexes were studied.

3. The platinum complex with an acceptor-donor-acceptor structure exhibited blue-shifted excimer's emission than that with a donor-acceptor structure in the neat film as evident from their photoluminescence spectra.

4. Both platinum complexes displayed excellent photoluminescent quantum efficiency.

5. The fabricated PLEDs exhibited stable white electroluminescent properties.

Novel Cyclometalated Platinum (II) Complex Containing Carrier-Transporting Groups: Synthesis, Luminescence and Application in Single-dopant White PLEDs

Aihui Liang [a,b], Yanhu Li [b], Weiguo Zhu [a*], Yafei Wang [a], Fei Huang [b],
Hongbin Wu [b], Yong Cao [b]

[a] *College of Chemistry, Key Lab of Environment-Friendly Chemistry and Application of the Ministry of Education, Xiangtan University, Xiangtan 411105, China*

[b] *Institute of Polymer Optoelectronic Materials & Devices, State Key Laboratory of Luminescent Materials and Devices, South China University of Technology, Guangzhou 510640, China*

Corresponding author: Dr. Weiguo Zhu

Tel: +86-731-58298280

Fax: +86-731-58292251

E-mail addresses: zhuwg18@126.com

ABSTRACT: In order to investigate the influence of carrier-transporting groups on the luminescent properties, especially on excimer/aggregation emission, and to obtain single emissive dopants used in white polymer light-emitting diodes with a single emissive-layer structure, two novel platinum complexes derived from a platinum(II) (2-(4′,6′-difluorophenyl)pyridinato-N,$C^{2\prime}$)(picolinate) unit containing carrier-transporting groups were synthesized and characterized, where a triphenylamino or an oxadiazole-triphenyl-amino functionalized unit was pending into the picolinate by non-conjugated linkage, respectively. Their opto-physical, electrochemical and electroluminescent properties were investigated. Compared to their parent platinum complex, both functionalized platinum complexes exhibited a significantly red-shifted photoluminescent profile in neat film and higher photoluminescent quantum efficiency in dichloromethane at room temperature. Furthermore, the platinum complex with oxadiazole-triphenylamino ambipolar transporting group exhibited better photoluminescent properties and offered potential application as a single dopant in a single-emissive-layer-based white polymer light-emitting diode. More stable white light emissions were observed in this platinum complex-doped devices at dopant concentrations of 4-8 wt%. The maximum luminous efficiency of 1.01 cd A^{-1} and the maximum brightness of 2177 cd m^{-2} were obtained in the polyfluorene-hosted devices.

Keywords: Electrophosphorescence; Platinum (II) complex; White polymer light-emitting devices; Synthesis

1. Introduction

White organic and polymeric light-emitting devices (WOLEDs/WPLEDs) have attracted a great deal of attention because of their potential applications in full color displays, back lighting of flat-panel displays and solid-state lighting [1-4]. To date, white light emission based on polymers and small molecules have been obtained by several methods and technologies [5–14]. There were two device structures to build the small molecule-based WOLEDs by sequential deposition; one is multiple-emissive-layer (MEL) structure **[**15-21**]** and the other is single-emissive-layer (SEL) structure [22-24]. However, these WOLEDs fabricated by deposition exhibited problems, such as complicated processes, high cost and poor stability. In order to overcome such problems, WOLEDs and WPLEDs fabricated by solution-processing technique were recently developed, in which all small organic molecules and polymers used as emitters were dissolved in the given solvents and spin-coated to form an emissive layer [25-31].

Using the solution processing technique, some high-performance white-emitting devices were achieved by a spin-coating process. For example, Wu *et al* [32] obtained a WPLED with a power efficiency (*PE*) of 20.3 lm W^{-1} and a luminescent efficiency (*LE*) of 42.9 cd A^{-1}, in which the blue-emitting small molecules of iridium complexes were spin-coated to form SEL with a blend of poly(N-vinylcarbazole) (PVK) and 2,2'-(1,3-phenylene)bis[5-(4-*tert*-butyl- phenyl)-1,3,4-oxadiazole] (OXD-7). Jen *et al* [33] made a WOLED containing PVK, OXD-7, the blue-emitting FIrpic, the green-emitting $Ir(ppy)_3$ and the red-emitting Os-R1 in SEL, which exhibited a maximum external quantum efficiency (*EQE*) of 5.85 %, a *PE* of 6.15 lm W^{-1} and a *LE* of 10.9 cd A^{-1}. Nevertheless, this class of devices, blending various emitters in the SEL structure, could have poor stability and can barely obtain a pure white emission due to phase separation and undesired Förster energy transfer from the high- energy emitter to the low-energy one. In order to decrease the emitter types in the SEL WOLEDs/WPLEDs, a class of emitters used as a single dopant was recently developed, which could present not only high-lying monomer emission, but also low-lying excimer emission in the devices. Meanwhile, our group reported some mononuclear platinum complexes and iridium complexes, as well as dinuclear platinum complexes as single emissive dopants in the SEL-based WPLEDs [34]. However, to our best knowledge, the platinum complex containing ambipolar transport groups has not yet been reported in the spin-coated WPLEDs using a single dopant [35].

As triphenylamine (TPA) and oxadiazole (OXD) are well-known hole- and electron-transporting moieties, respectively, applied in the fields of OLEDs and organic solar cells [36], they can form ambipolar transport groups and are suggested to be available to improve the optoelectronic properties of their resulting platinum complexes while they are simultaneously introduced into the platinum complex as substituent groups. In order to investigate the influence of the ambipolar transport groups on the luminescent properties, especially on excimer/aggregation emission of these platinum complexes and further to obtain a class of single emissive dopants used in the SEL-based WPLEDs, a novel platinum complex with ambipolar transporting groups of TPA and OXD, i.e. FPt(OXD6TPA6Pic), was designed and synthesized, where FPt is a platinum(II) (2-(4′,6′-difluorophenyl) pyridinato-N,$C^{2\prime}$) unit, and OXD6TPA6Pic is an oxadiazole-triphenylamino functionalized picolinate, respectively. For comparison, another platinum complex with only a hole-transporting group of TPA, i.e. FPt(TPA6Pic), was also synthesized, where TPA6Pic is a triphenylamino functionalized picolinate. The photophysical, electrochemical and thermal properties, as well as electroluminescent properties for both platinum (II) complexes were studied. As expected, the pending carrier transporting groups have exhibited a significant influence on the luminescent properties of their corresponding platinum complexes. The FPt(OXD6TPA6Pic) with ambipolar transport groups can be used as a single dopant to obtain WPLEDs containing a polymer matrix of PVK or poly(9,9-dihexylfluorene) (PFO), respectively. The best device performance with a maximum *LE* of 1.0 cd/A and brightness of 855 cd/m^2 was obtained in the FPt(OXD6-TPA6Pic)-doped PFO device at dopant concentrations of 8 wt% and a white emission with a stable CIE coordinate of (0.30, 0.38) was observed at the same time.

2. Experimental Section

2.1. Materials and equipment

All solvents were carefully dried and distilled prior to use. Commercially available reagents were used without further purification unless otherwise stated. 3-(6-(4-(Diphenyl-amino)benzyloxy)hexyloxy)picolinic acid (TPA6PicH) and 3-(6-(4'-((4-((6-(4-(5-(4-methyl)-1,3,4-oxadiazole-2-yl)phenoxy)hexyloxy)methyl)phenyl)(phenyl) amino) biphen-yl-4-yloxy)hexyloxy)picolinic acid (OXD6TPA6PicH) were prepared according to the reported process, respectively [37]. For further comparison, platinum (II) (4′,6′-(difluoro-phenyl) pyridinato-N,C2′) (picolinate) [FPt(pic)] was also made based on our previous work [34]. All reactions were performed under nitrogen atmosphere and were monitored by thin-layer chromatography (TLC). Flash column chromatography and preparative TLC were carried out using silica gel from Merck (200-300 mesh). All ^{1}H NMR spectra were acquired at a Bruker Dex-400NMR instrument using $CDCl_3$ as a solvent. Elemental analysis was performed on a Harrios elemental analysis instrument. Time-of-flight mass spectrometry (TOF-MS) was performed in the positive ion mode with a matrix of dithranol at a Bruker-autoflex III smartbeam. The UV absorption and photoluminescence (PL) spectra were measured with a Varian Cray50 and Perkin-Elmer LS50B Luminescence Spectrometer, respectively. EL spectra and CIE coordinates were recorded with an Insta-Spec IV CCD system (Oriel). Luminance and luminous efficiency-current density (*LE*–*J*) data were measured with a Si photodiode and calibrated by using a PR-705 spectrascan spectrophotometer (Photo Research).

2.2 Synthesis of FPt(TPA6Pic)

To a mixture of K_2PtCl_4 (0.3 g, 0.84 mmol) and water (5 mL) was added 2-(2,4-difluorophenyl)pyridine (0.4 g, 2.1 mmol) and 2-ethoxyethanol (15 mL). The mixture was stirred vigorously at 100 ^{o}C under inert gas atmosphere for 20 h. After cooling to room temperature (RT), the colored precipitate was filtered off, washed with water and hexane, respectively. A red solid of dimer of $[FPtCl]_2$ was obtained (0.42 g, 78.0 %). Then a mixture of the dimer (0.2 g, 0.24 mmol), compound TPA6PicH (0.30 g, 0.60 mmol) and sodium carbonate (90 mg, 0.85 mmol) in 2-ethoxyethanol (15 mL) at about 80-90 ^{o}C was stirred vigorously under inert gas atmosphere for 24 h. After cooling to RT, the mixture was extracted with dichloromethane (CH_2Cl_2) and the resulting organic layer was dried over anhydrous magnesium sulfate. The solvent was removed and the residue was purified by a dry flash silica gel column using CH_2Cl_2 as eluent to gain FPt(TPA6Pic) (0.22 g, 53.0 %) as a brown red solid. ^{1}H NMR ($CDCl_3$, 400 MHz), δ (ppm): 9.14-9.15 (d, *J* = 4.8 Hz, 1H), 8.63-8.64 (d, *J* = 5.2 Hz, 1H), 7.97-7.99 (d, *J* = 5.8 Hz, 1H), 7.86-7.89 (t, 1H), 7.65-7.67 (d, *J* = 5.4 Hz, 1H), 7.52-7.53 (t, 1H), 6.85-7.21 (m, 15H), 6.84-6.86 (d, *J*

= 5.8 Hz, 1H), 6.58-6.59 (t, 1H), 4.42 (s, 2H), 4.16-4.18 (t, 2H), 3.49-3.52 (t, 2H), 1.96-2.03 (m, 2H), 1.90-1.92 (m, 2H), 1.63-1.65 (m, 2H), 1.47-1.50 (m, 2H). ^{13}C NMR (100 MHz, $CDCl_3$) δppm: 170.11, 158.09, 149.89, 147.85, 147.26, 141.39, 139.54, 132.97, 129.20, 128.85, 128.14, 125.12, 124.16, 124.02, 122.70, 114.63, 114.45, 99.50, 70.39, 67.65, 29.16, 28.81, 25.76, 25.53. Anal. Calcd for $C_{42}H_{37}F_2N_3O_4Pt$: C 57.27, H 4.23, N 4.77. Found: C 57.32, H 4.20, N 4.81. MALDI-TOF (m/z): calcd for $[M]^+$ 880.24, found $[M]^+$ 880.20.

2.3 Synthesis of FPt(OXD6TPA6Pic)

This was prepared according to the synthetic procedure of FPt(TPA6Pic). A brown red solid was obtained with a yield of 36.0 %. ^{1}H NMR ($CDCl_3$, 400 MHz), δ (ppm): 9.19-9.20 (d, *J* = 5.2 Hz, 1H), 8.66-8.68 (d, *J* = 5.4 Hz, 1H), 8.00-8.06 (m, 5H), 7.85-7.87 (t, 1H), 7.78-7.76 (d, *J* =5.8 Hz, 1H), 7.52-7.58 (m, 1H), 7.46-7.48 (d, *J* = 8.5 Hz, 2H), 7.40-7.42 (d, *J* = 8.4 Hz, 2H), 7.32-7.34 (d, *J* = 8.0 Hz, 2H), 7.23-7,27 (t, 4H), 7.16-7.18 (t, 1H), 7.08-7.12 (m, 6H), 7.00-7.02(d, *J* = 8.8 Hz, 3H), 6.93-6.95 (d, *J* = 8.4 Hz, 2H), 6.76-6.77 (d, *J* = 6.4 Hz, 1H), 6.54-6.60 (t, 1H), 4.46 (s, 2H), 4.20-4.21 (t, 2H), 4.01-4.06 (t, 4H), 3.51-3.55 (t, 2H), 2.45 (s, 3H), 1.99-2.05 (m, 2H), 1.84-1.87 (m, 4H), 1.61-1.78 (m, 10H). ^{13}C NMR (100 MHz, $CDCl_3$) δppm: 170.21, 164.37, 164.27, 161.88, 158.41, 150.04, 147.74, 147.22, 146.47, 142.01, 141.33, 139.66, 135.16, 133.01, 132.90, 129.24, 128.89, 128.65, 127.64, 126.80, 124.23, 116.36, 114.98, 114.83, 99.68, 72.71, 70.36, 68.18, 67.84, 29.73, 29.18, 29.14, 26.05, 25.92, 25.49, 21.66. Anal. Calcd for $C_{69}H_{63}F_2N_5O_7Pt$: C 63.39, H 4.86, N 5.36. Found: C 63.42, H 4.87, N 5.32. MALDI-TOF (m/z): calcd for $[M]^+$ 1306.43, found $[M]^+$ 1306.38.

2.4 Fabrication of PLEDs

The devices were made based on the following standard procedure. The ITO glass substrate was cleaned by ultrasonic bath sequentially in acetone, detergent, deionized water and isopropanol, and baked at 80 ^oC. A 40 nm-thick layer of poly(ethylendioxy-thiophene):poly(styrene sulfonic acid) (PEDOT:PSS, Baytron P4083, Bayer AG) was spin-coated onto the precleaned ITO-glass substrates after an O_2 plasma treatment and dried in vacuum box for over 8 h. In the PFO-hosted devices, a 40 nm thick layer of PVK (10 mg/mL in dichlorobenzene) was spin-coated on the top of PEDOT and baked at 120 ^oC for 30 min. Then a mixture of the platinum complex with PVK+PBD (or PFO) was respectively spin-coated onto the top of PPEDOT (or PVK) to form the emitting layer from the solution in chlorobenzene (or in p-xylene) at a concentration of 20 mg/mL by adapted rotate speed and baked at 120 ^oC for 20 minutes. The thickness of all spin-coated films was measured by Profilometer (Tencor Alfa-Step 500). Finally, a thin layer of CsF (1.5 nm) with about 120 nm thick Al capping layer was deposited through a shadow mask in a vacuum chamber under a base pressure of ~10^{-4} Pa. The deposited thickness was monitored by a crystal thickness monitor (Sycon). The devices were made in a controlled atmosphere dry-box (Vacuum Atmosphere Co.) in N_2 atmosphere except processing PEDOT:PSS layer. The active area was 0.19 cm^2 and five parallel measurements were performed for each device.

3. Results and discussion

3.1. Synthesis

As shown in **Scheme 1**, the platinum (II) complexes of FPt(TPA6Pic) and FPt(OXD6-TPA6Pic) were synthesized by two-step procedures, which commenced from the reaction of K_2PtCl_4 with 2,4-difluoropyphenylpyridine and a chloride cleavage of the resulting chloro-bridged dimer with either TPA6PicH or OXD6TPA6Pic under moderate conditions based on the reported procedures [38-40], respectively. Since the ancillary ligand OXD6TPA6PicH offers larger steric hindrance than TPA6PicH, the resulting platinum complex of FPt(OXD6TPA6Pic) is more difficult to obtain and has a lower yield than FPt(TPA6Pic). Both platinum complexes were confirmed by ^{1}H NMR, ^{13}C NMR, elemental analysis and TOF-MS.

3.2. Optical Analysis

Figure 1 shows the UV-vis absorption spectra of FPt(OXD6TPA6Pic), FPt(TPA6Pic) and FPt(pic) [platinum (II) (4′,6′-(difluorophenyl) pyridinato-N,C2′) (picolinate)] in CH_2Cl_2 at 298 K, and their UV absorption data are summarized in **Table 1**. An intense high-energy absorption band at about 304 nm and a moderate low-energy absorption band at 350 nm were observed for these functionalized platinum complexes with carrier-transporting groups, in which the former band is assigned to the intraligand-based π-π* transitions and the latter band is assigned to the mixing transitions between the spin-allowed singlet metal-to-ligand charge transfer (^{1}MLCT) and the spin- forbidden triplet metal-to-ligand charge transfer (^{3}MLCT) [34]. Compared to the parent platinum complex of FPt(pic), both functionalized platinum complexes of FPt(TPA6Pic) and FPt(OXD6TPA6Pic) exhibited an additional strong high-lying absorption bands at about 305 nm, which is attributed to the absorption from the fluorescent chromophores of TPA and/or OXD [41,42].

The PL spectra of these platinum complexes are shown in **Figure 2a**, and their emission data are summarized in **Table 1**. Nearly identical PL profiles containing a maximum emission peak at 462 nm with a shoulder at 506 nm are exhibited for both FPt(TPA6Pic) and FPt(OXD6TPA6Pic) in CH_2Cl_2 solution. Compared to FPt(Pic), both functionalized platinum complexes displayed a wider PL profile due to the intrinsic emission's influence of the pending donor unit of triphenylamino and acceptor unit of oxadiazole in the picolinate. Furthermore, FPt(OXD6TPA6Pic) exhibited wider PL spectrum than FPt(TPA6Pic), which should be attributed to the additional effect of the oxadiazole' emission in dilute CH_2Cl_2 solution.

Figure 2b shows the PL spectra of these three platinum complexes in their neat films. An obviously red-shifted low-energy emission peak over 600 nm is observed, which is attributed to the planar molecular configuration of platinum complexes leading to excimer formation [43]. The maximum emission peaks of the proposed eximers are located at 681 nm for FPt(TPA6Pic) and 650 nm for FPt(OXD6TPA6Pic), respectively. Both functionalized platinum complexes displayed a significantly red-shifted PL spectra compared to FPt(Pic) in the neat films. The significantly red-shifted excimer emissions for FPt(TPA6Pic) and FPt(OXD6TPA6Pic) should result from their additional inter-molecular interaction through the space between donor and acceptor units. Interestingly, FPt(OXD6TPA6Pic) exhibited a 31 nm blue-shifted PL spectrum than FPt(TPA6Pic) in its neat film due to the electron-withdrawing effect of OXD under this state. The diference of PL profile between in solution and in film indicates that intermolecular interaction through the space between donor and acceptor units mainly exists in the film. The salvation effect can efficiently restrain the intermolecular donor-acceptor interaction.

To further investigate the effect of carrier-transporting groups in ancillary ligands on the PL performances of their platinum complexes, their fluorescence quantum yields (Φ_f) were measured using 9,10-diphenylanthrancene as the standard ($\Phi_f = 0.9$) in degassed CH_2Cl_2 under photo-excitation at 380 nm [44]. As shown in **Table 1**, the Φ_f of 0.74 for

FPt(TPA6Pic), 0.81 for FPt(OXD6TPA6Pic**)** and 0.58 for FPt(pic) were obtained in CH_2Cl_2, respectively. It is obvious that both functionalized platinum complexes displayed a higher Φ_f than the parent FPt(pic). Therefore, introducing carrier-transporting groups into the ancillary ligand is a means to improve the luminescence efficiency of its resulting platinum (II) complexes in CH_2Cl_2. Interestingly, for these functionalized platinum complexes, the FPt(OXD6TPA6Pic) with ambipolar transporting groups of TPA and OXD has the higher Φ_f than the FPt(TPA6Pic) with only hole transporting group.

3.3 Thermal Property

The thermal stability of platinum complexes was evaluated by thermogravimetric analysis (TGA) under N_2 stream with a scanning rate of 20 ^{o}C/min, and their degradation temperatures (T_d) for 5% weight loss are listed in **Table 2**. The recorded T_d level is 253 ^{o}C for FPt(TPA6Pic), 264 ^{o}C for FPt(OXD6TPA6Pic) and 294 ^{o}C for FPt(Pic), respective -ly. It indicates that these functionalized platinum complexes possess good thermal property. Compared to FPt(Pic), FPt(TPA6Pic) and FPt(OXD6TPA6Pic) showed a lower decomposition temperature because of a non-conjugating linkage between the parent picolinic acid and the pending carrier-transporting groups.

3.4. Electrochemical Property

The electrochemical behavior of the three cyclometalated platinum complexes was measured by cyclic voltammetry using ferrocene as the internal standard and their data are listed in **Table 2**. Irreversible oxidation peaks presented from −1.61V to −2.29 V for these platinum complexes. On the basis of these onset oxidation potentials (E_{ox}) and the formula of $E_{\mathrm{HOMO}} = -(E_{\mathrm{ox}} + 4.34)$ eV, the highest occupied molecular orbital energy levels (E_{HOMO}) were calculated to be − 5.95 eV for FPt(TPA6Pic) and − 6.03 eV for

FPt(OXD6TPA6Pic), respectively. As the reduction peak was not displayed, the lowest unoccupied molecular orbital energy levels (E_{LUMO}) had to be calculated based on the equation of $E_{\mathrm{LUMO}} = E_{\mathrm{HOMO}} + E_{\mathrm{g}}$, in which energy band gap (E_{g}) was estimated from the UV-vis absorption threshold [45]. As a result, the E_{LUMO} was − 3.04 eV for FPt(TPA6Pic) and − 3.09 eV for FPt(OXD6TPA6Pic) were obtained. Apparently, the pending carrier-transporting groups have an important influence on the HOMO and LUMO energy levels of their platinum complexes. Both functionalized platinum complexes exhibited an increasing E_{LUMO} and E_{LUMO} value compared to the parent FPt(Pic) due to the effect of the carrier-transporting groups. Furthermore, FPt(OXD6TPA6Pic) displayed a decreased E_{LUMO} and E_{LUMO} value compared to FPt(TPA6Pic) due to the effect of the OXD acceptor unit.

3.5. Electroluminescent Property

To investigate the influence of ambipolar transporting group on electroluminescence (EL) properties of its platinum complex, FPt(OXD6TPA6Pic) was chosen as the single dopant in the devices. The SEL-based devices were fabricated with a structure of ITO/ PEDOT:PSS (40 nm)/dopant + PVK-PBD (70 nm)/CsF(1.5 nm)/Al (120 nm) (devices A) and ITO/PEDOT:PSS (40 nm)/PVK (40 nm)/dopant + PFO (70 nm)/CsF(1.5 nm)/Al (120 nm) (devices B). The emitting layer consist of the FPt(OXD6TPA6Pic) dopant and polymeric host matrix of PFO or PVK-PBD blend, in which the weight concentration of the dopant is 4 and 8 wt %, PBD weight ratio is 30 wt % in the PVK-PBD blend, respectively. The energy bands of FPt(OXD6TPA6Pic), PVK, PFO and PBD are shown in the supplementary information accompanying this work (**Figure S2**).

Figure 3 showed the EL spectra of the PVK-hosted devices A and the PFO-hosted devices B at different dopant concentrations of 4 wt % and 8 wt % at 12 V. All of these EL spectra exhibited a broad emission band from 400 to 750 nm. For devices A, three emission peaks at 438, 484, 516 nm and a shoulder at 544 nm were observed. For devices B, four emission peaks at 421, 439, 481, 511 nm and a shoulder at 540 nm were observed. In these emission peaks, the high-lying emission peaks below 450 nm are assigned to the host matrix, the low-lying emission peaks in a range of 450-520 nm are attributed to intrinsic emission of FPt(OXD6TPA6Pic). Additionally, the shoulder in the low-lying region, according to the reports by Chen *et al* [46], is attributed to the electromers between host matrix and dopant. Compared to the PL spectra in the neat film, however, little excimer emission at about 650 nm can be observed in the EL spectra for the PFO-hosted devices B at 8 wt% dopant concentration. This implies that the excimer emission from the platinum complexes can be efficiently tuned by the pendant ambipolar transporting groups in their ancillary ligands under an electric field.

It was noted that the contribution between the host matrix and the FPt(OXD6TPA6Pic) guest on the EL spectra is significantly different in the devices A and devices B. The emission intensity from host matrix for PFO is much stronger than that for PVK. This feature suggests that the energy transfer is more incomplete from the PFO instead of PVK-PBD matrix to FPt(OXD6-TPA6Pic). The incomplete energy transfer can be used to obtain a white emission in the FPt(OXD6TPA6Pic)-doped PFO devices. **Figure 3** inset shows the Commission Internationale de L’Eclairage (CIE) coordinates for these devices. The devices B displayed more efficient white light emission than the devices A. In order to investigate the EL stability of the devices, the EL spectra of the devices B at the dopant concentration of 8 wt % was measured under different applied voltages, as shown in

Figure S3. A minor change for the EL CIE coordinates from (0.29, 0.39) to (0.30, 0.38) is observed with the increasing driving voltages from 8 V to 13 V. Therefore, the devices B exhibited stable white emission under different driving voltages.

Figure 4 shows the luminous efficiency-current density-luminance (*LE*-*J*-*L*) characteristics of the devices A and devices B. **Table 3** summarizes the performance of these devices at 4 wt% and 8 wt% dopant concentrations. The near-white emissions with the CIE coordinates (0.28 ± 0.04, 0.40 ± 0.08) were observed for these FPt(OXD6TPA6 -Pic)-doped devices at a applied voltage of 12V. The maximum *LE* of 1.01 cd A^{-1} at a current density of 3.20 mA cm^{-2} and the maximum brightness of 2177 cd m^{-2} were obtained in the PFO-hosted devices B, respectively. For the recorded maximum *LE* and brightness, the devices B exhibited higher levels than the devices A. At this time, the CIE coordinates located at the near-white, even white region range from (0.24, 0.32) to (0.30, 0.38) at the dopant concentrations of 4 wt% ~ 8 wt% for the devices B at 12V. This indicates that PFO is a better host matrix than PVK-PBD for the FPt(OXD6TPA6Pic)-doped devices to obtain high-performance WPLEDs.

4. Conclusion

In summary, two novel cyclometalated platinum complexes, FPt(OXD6TPA6Pic) and FPt(TPA6Pic), containing carrier-transporting groups were obtained. Both functionalized platinum complexes exhibited significantly red-shifted excimer emission in neat film and increased PL quantum efficiency in CH_2Cl_2 solution compared to the parent FPt(pic). Furthermore, the FPt(OXD6TPA6Pic) containing ambipolar transporting groups exhibited better PL property and potential application used as a single dopant in the SEL WPLEDs. Stable white light emissions were observed in the FPt(OXD6TPA6Pic)-doped

PFO devices at the dopant concentrations of 4 wt% ~ 8 wt% and different driving voltages of 8V~13V. The maximum *LE* of 1.01 cd A^{-1} and the maximum brightness of 2177 cd m^{-2} were obtained, respectively. The results demonstrated that introducing the ambipolar transporting groups of TPA and OXD into the ancillary ligand can lead to beneficial properties for the constructing platinum complex in the SEL-based WPLEDs.

Acknowledgements

Financial support from the National Natural Science Foundation of China (50973093, 51273168 and 21202139), the Innovation Group in Hunan Natural Science Foundation (12JJ7002), the Specialized Research Fund and the New Teachers Fund for the Doctoral Program of Higher Education of China (20094301110004), the Scientific Research Fund of Hunan Provincial Education Department (10A119, 11CY023, 10B112), Natural Science Foundation of Hunan (12JJ4019), and the Scientific Research Fund of Xiangtan University (11QDZ18, 2011XZX08), Postgraduate Science Foundation for Innovation in Hunan Province (CX2011B263).

References

[1] Che CM, Chan SC, Xiang HF, Chan MCW, Liu Y, Wang Y. Tetradentate schiff base platinum(II) complexes as new class of phosphorescent materials for high-efficiency and white-light electroluminescent devices. Chem Commun 2004; 1484-6.

[2] Kamtekar KT, Monkman AP, Bryce MR. Recent advances in white organic light-emitting materials and devices. Adv Mater 2010; 22: 572-82.

[3] Park YS, Kang JW, Kang DM, Park JW, Kim YH, Kwon SK, Kim JJ. Efficient, color stable white organic light-emitting diode based on high energy level yellowish-green dopants. Adv Mater 2008; 20: 1957 - 61.

[4] Holder E, Langeveld BMW, Schubert US. New trends in the use of transition metal-ligand complexes for applications in electroluminescent devices. Adv Mater 2005; 17: 1109 -21.

[5] Zhao ZJ, Zhao YX, Lu P, Tian WJ. Fluorene-centered, ethynylene-linked carbazole oligomers: synthesis, photoluminescence, and electroluminescence. J Phys Chem C 2007; 111: 6883-8.

[6] Mazzeo M, Vitale V, Della Sala F, Anni M, Barbarella G, Favaretto L, Sotgiu G, Cingolani R, Gigli G. Bright white organic light-emitting devices from a single active molecular material. Adv Mater 2005; 17: 34-9.

[7] a) Niu QL, Shao YX, Xu W, Wang L, Han SH, Liu NL, Peng JB, Cao Y, Wang J. Full color and monochrome passive-matrix polymer light-emitting diodes flat panel displays made with solution processes. Org Electron 2008; 9: 95-100. b) D'Andrade BW, Forrest SR. white organic light-emitting devices for solid-state lighting. Adv Mater 2004; 16: 1585-95. c) Kalinowski J, Fattori V, Cocchi M, Williams JAG. Light-emitting devices based on organometallic platinum complexes as emitters. Coord Chem Rev 2011; 255: 2401-5. d) Duggal R, Shiang JJ, Heller CM, Foust DF. Local electric-field-driven repoling reflected in the ferroelectric polarization of Ce-doped $Sr_{0.61}Ba_{0.39}Nb_2O_6$. Appl Phys Lett 2002; 80: 470-2. e) Paik KL, Baek NS, Kim HK, Lee JH, Lee Y. White light-emitting diodes from novel silicon-based copolymers containing both electron-transport oxadiazole and hole-transport carbazole moieties in the main chain. Macromolecules 2002; 35: 6782-91. f) Li SF, Zhong GY, Zhu WH, Li FY, Pan JF, Huang W, Tian H. Dendritic europium complex as a

single dopant for white-light electroluminescent devices. J Mater Chem 2005; 15: 3221-8.

[8] Sun Y, Giebink NC, Kanno H, Ma B, Thompson ME, Forrest SR. Management of singlet and triplet excitons for efficient white organic light-emitting devices. Nature 2006; 440: 908-12.

[9] D'Andrade BW, Brooks J, Adamovich V, Thompson ME, Forrest SR. White light emission using triplet excimers in electrophosphorescent organic light-dmitting devices. Adv Mater 2002; 14: 1032-6.

[10] Zhang Y, Huang F, Jen AKY, Chi Y. High-efficiency and solution processible multilayer white polymer light-emitting diodes using neutral conjugated surfactant as an electron injection layer. Appl Phys Lett 2008; 92: 063303 - 5.

[11] D'Andrade BW, Thompson ME, Forrest SR. Controlling exciton diffusion in multilayer white phosphorescent organic light emitting devices. Adv Mater 2002; 14: 147-51.

[12] Chen L, Li PC, Cheng YX, Xie ZY, Wang LX, Jing XB, Wang FS. White electroluminescence from star-like single polymer systems: 2,1,3-benzothiadiazole derivatives dopant as orange cores and polyfluorene host as six blue arms. Adv Mater 2011; 23: 2986-90.

[13] Wu HB, Ying L, Yang W, Cao Y. Progress and perspective of polymer white light-emitting devices and materials. Chem Soc Rev 2009; 38: 3391-400.

[14] Thompson J, Blyth RIR, Mazzeo M, Anni M, Gigli G, Cingolani R. White light emission from blends of blue-emitting organic molecules: A general route to the white organic light-emitting diode. Appl Phys Lett 2001; 79: 560-2.

[15] Yu XM, Kwok HS, Wong WY, Zhou GJ. High-efficiency white organic light-emitting devices based on a highly amorphous iridium(III) orange phosphor. Chem Mater 2006; 18: 5097-103.

[16] Yu XM, Zhou GJ, Lam CS, Wong WY, Zhu XL, Sun JX, Wong M, Kwok HS. A yellow-emitting iridium complex for use in phosphorescent multiple-emissive-layer white organic light-emitting diodes with high color quality and efficiency. J Organomet Chem 2008; 693: 1518-27.

[17] Sasabe H, Takamatsu JI, Motoyama T, Watanabe S, Wagenblast G, Langer N, Molt

O, Fuchs E, Lennartz C, Kido J. High-efficiency blue and white organic light-emitting devices incorporating a blue iridium carbene complex. Adv Mater 2010; 22: 5003-7.

[18] Rehmann N, Ulbricht C, Köhnen A, Zacharias P, Gather MC, Hertel D, Holder E, Meerholz K, Schubert US. Advanced device architecture for highly efficient organic light-emitting diodes with an orange-emitting crosslinkable iridium(III) complex. Adv Mater 2008; 20: 129-33.

[19] Tian N, Thiessen, A, Schiewek R, Schmitz OJ, Hertel D, Meerholz K, Holder E. Efficient synthesis of carbazolyl- and thienyl-substituted beta-diketonates and properties of their red and green light-emitting Ir(III) complexes. J Org Chem 2009; 74: 2718-25.

[20] Ulbricht C, Rehmann N, Holder E, Hertel D, Meerholz K, Schubert US. Synthesis and characterization of oxetane-functionalized phosphorescent Ir(III) complexes. Macromol Chem Phys 2009; 210: 531-41.

[21] Tian N, Lenkeit D, Pelz S, Kourkoulos D, Hertel D, Meerholz K, Holder E. Screening structure-property-correlations and device performance of Ir(III) complexes in multi-layer PhOLEDs. Dalton Trans 2011; 40: 11629-35.

[22] a) D'Andrade BW, Holmes RJ, Forrest SR. Efficient organic electrophosphorescent white-light-emitting device with a triple doped emissive layer. Adv Mater 2004; 16: 624 - 8. b) Cheng G, Li F, Duan Y, Feng J, Liu SY, Qiu S, Lin D, Ma YG, Lee ST. White organic light-emitting devices using a phosphorescent sensitizer. Appl Phys Lett 2003; 82: 4224-6.

[23] D’Andrade BW, Baldo MA, Adachi C, Brooks J, Thompson ME, Forrest SR. High-efficiency yellow double-doped organic light-emitting devices based on phosphor-sensitized fluorescence. Appl Phys Lett 2001; 79: 1045-7.

[24] Tian N, Aulin YV, Lenkeit D, Pelz S, Mikhnenko OV, Blom PWM, Loi M A, Holder E. Cyclometalated red iridium(III) complexes containing carbazolyl-acetyl-acetonate ligands: efficiency enhancement in polymer LED devices. Dalton Trans 2010; 39: 8613-5.

[25] Misra A, Kumar P, Kamalasanan MN, Chandra S. White organic LEDs and their recent advancements. Semicond Sci Technol 2006; 21: R35-47.

[26] Kido J, Hongawa K, Okuyama K, Nagai K, White light-emitting organic electroluminescent devices using the poly(N-vinylcarbazole) emitter layer doped with three fluorescent dyes. Appl Phys Lett 1994; 64: 815-7

[27] Tekin E, Holder E, Marin V, de Gans BJ, Schubert US, Inkjet printing of luminescent ruthenium- and iridium-containing polymers for applications in light-emitting devices. Macromol Rapid Commun 2005; 26: 293-7.

[28] Marin V, Holder E, Wienk MM, Tekin E, Kozodaev D, Schubert US. Inkjet printing of electron donor/acceptor blends: towards bulk heterojunction solar cells. Macromol Rapid Commun 2005; 26: 319-24.

[29] Marin V, Holder E, Hoogenboom R, Tekin E, Schubert US. Light-emitting iridium(III) and ruthenium(II) polypyridyl complexes containing quadruple hydrogen -bonding moieties. Dalton Trans 2006; 13: 1636-44.

[30] Tekin E, Wijlaars H, Holder E, Egbe DAM, Schubert US. Film thickness dependency of the emission colors of PPE-PPVs in the inkjet printed libraries. J Mater Chem 2006; 16: 4294-8.

[31] Tekin E, Holder E, Kozodaev D, Schubert US. Controlled pattern formation of MEH-PPV by inkjet printing. Adv Funct Mater 2007; 17: 277-84.

[32] Wu HB, Zhou GJ, Zou JH, Ho CL, Wong WY, Yang W, Peng JB, Cao Y. Efficient polymer white-light-emitting devices for solid-state lighting. Adv Mater 2009; 21: 4181-4.

[33] Niu YH, Liu MS, Ka JW, Bardeker J, Zin MT, Schofield R, Chi Y, Jen AKY. Crosslinkable hole-transport layer on conducting polymer for high-efficiency white polymer light-emitting diodes. Adv Mater 2007; 19: 300-4.

[34] a) Wang YF, Liu Y, Li XS, Qi HR, Zhu MX, Wang L, Lei GT, Wei QL, Zhu WG, Peng JB, Cao Y. Novel cyclometalated platinum (II) complex containing alkyl-trifluorene picolinic acid as emitter for single-layer white PLEDs. Org Electron 2010; 11: 1954 - 9. b) Li XS, Wang YF, Liu M, Ni MJ, Zhang ZY, Liu Y, Luo J, Shi DY, Chen Q, Lei GT, Zhu WG. Synthesis and opto-electronic properties of a dinuclear Pt(II)-Ir(III) complex bridged with bipicolinic acid derivative. Dalton Trans 2012; 41: 2972-8.

[35] Furuta PT, Deng L, Garon S, Thompson ME, Fre´chet JMJ. Platinum-functionalized

random copolymers for use in solution-processible, efficient, near-white organic light-emitting diodes. J Am Chem Soc 2004; 126: 15388-9.

[36] a) Shu CF, Dodda R, Wu FI, Liu MS, Jen AKY. Highly efficient blue-light-emitting diodes from polyfluorene containing bipolar pendant groups. Macromolecules 2003; 36: 6698-703. b) Xu ZW, Li Y, Ma XM, Gao XD, Tian H. Synthesis and properties of iridium complexes based 1,3,4-oxadiazoles derivatives. Tetrahedron. 2008; 64: 1860-7.

[37] Karakus C, Fischer LH, Schmeding S, Hummel J, Risch N, Schäferling M, Holder E. Oxygen and temperature sensitivity of blue to green to yellow light-emitting Pt(II) complexes. Dalton Trans 2012; 41: 9623-32.

[38] Fischer LH, Karakus C, Meier RJ, Risch N, Wolfbeis OS, Holder E, Schäferling M. Referenced dual pressure and temperature sensitive paint for color camera read out. Chem Eur J 2012; in press.

[39] Liang AH, Wang YF, Liu Y, Tan H, Cao YB, Li L, Li XS, Ma WJ, Zhu MX, Zhu WG. Synthesis, photophysical and electrochemical characterization of the hetero-leptic iridium complexes with modified ancillary ligand by carrier-transporting groups. Chin J Chem 2010; 28: 2455-62.

[40] Wang YF, Deng XP, Liu Y, Ni MJ, Liu M, Tan H, Li XS, Zhu WG, Cao Y. White emission from dinuclear cyclometalated platinum(II) complex in single-emitting layer PLEDs. Tetrahedron 2011; 67: 2118-24.

[41] Pu YJ, Kurata T, Soma M, Kido J, Nishide H. Triphenylamine- and oxadiazole-substituted poly(1,4-phenylenevinylene)s: synthesis, photo-, and electroluminescent properties. Synth Met 2004; 143: 207-14.

[42] Wu G L, Yang Y, He C, Chen XM, Li YF. A new triphenylamine-based hyper-branched polyfluorene with oxadiazole units on its side chains. Eur Polym J 2008; 44: 4047-53.

[43] Kozhevnikov VN, Donnio B, Bruce DW. Phosphorescent, terdentate, liquid-crystalline complexes of platinum(II): stimulus-dependent emission. Angew Chem Int Ed 2008; 47: 6286-9.

[44] Peng Q, Xu J, Li MJ, Zheng WX. Blue emitting polyfluorenes containing dendro-nized carbazole and oxadiazole pendants: synthesis, optical properties, and electro-

luminescent properties. Macromolecules 2009; 42: 5478- 85.

[45] Si ZJ, Li J, Li B, Hong ZR, Liu SY, Li WL. Electroluminescence from singlet excited-state of the exciplex between (2,3-dicarbonitrilopyrazino[2,3-f][1,10] phenan -throline) Re(CO)Cl and CBP. J Phys Chem C 2008; 112: 3920-5.

[46] Chen XW, Liao JL, Liang YM, Ahmed MO, Tseng HE, Chen SA. High-efficiency red-light emission from polyfluorenes grafted with cyclometalated iridium complexes and charge transport moiety. J Am Chem Soc 2003; 125: 636 – 7.

.

Table 1

The optophysical data of FPt(Pic), FPt(TPA6Pic) and FPt(OXD6TPA6Pic)

Compounds	UV-vis (nm)	Emission[a] (nm)	Emission[b] (nm)	Φ_{em} (%)
FPt(pic)	325, 350, 404	475, 502	601	0.58
FPt(TPA6Pic)	304, 351, 404	462, 506	681	0.74
FPt(OXD6TPA6Pic)	310, 348, 404	462, 506	650	0.81

[a]

Measured in DCM at room temperature;

[b] Measured in the neat film at room temperature.

Table 2

Electrochemical and thermal data of FPt(Pic), FPt(TPA6Pic) and FPt(OXD6TPA6Pic)

Compounds	HOMO (eV)	LUMO (eV)	E_g (eV)[a]	T_d(^{o}C)
FPt(pic)	-6.63	-3.46	3.17	294
FPt(TPA6Pic)	-5.95	-3.04	2.91	253
FPt(OXD6TPA6Pic)	-6.03	-3.09	2.94	264

[a] Estimated according to the UV-vis absorption spectrum.

Table 3

The performances of device A and B at different dopant concentrations of 4 wt % and 8 wt %

Devices	LE_{max}(cd/A)	V(V)[a]	J(mA/cm^2)[b]	L_{max}(cd/m^2)	$V_{turn-on}$(V)	CIE(x,y)[c]
A-4 wt%	0.80	8.0	1.1	318	6.4	0.30, 0.43
A-8 wt%	0.93	7.4	3.2	314	6.0	0.32, 0.48
B-4 wt%	0.82	7.4	3.9	2117	6.5	0.24, 0.32
B-8 wt%	1.01	7.8	1.8	855	6.4	0.30, 0.38

[a] Voltage at the maximum LE; [b] Current density at the maximum LE;
[c] Commission Internationale de L'Eclairage coordinates at 12 V.

Figure captions

Figure 1. Normalized UV-vis absorption spectra of FPt(OXD6TPA6Pic), FPt(TPA6Pic) and FPt(Pic) in CH_2Cl_2 at room temperature

Figure 2. Normalized PL spectra of FPt(OXD6TPA6Pic), FPt(TPA6Pic) and FPt(Pic) in CH_2Cl_2 (a), and their neat films at room temperature (b)

Figure 3. EL spectra of the devices A and B at different dopant concentrations of 4 wt % and 8 wt % at 12 V.

Figure 4. The luminous efficiency-current density-luminance (*LE*-*J*-*L*) characteristics of the devices A and devices B

Scheme 1. Synthetic route of FPt(TPA6Pic) and FPt(OXD6TPA6Pic)

Figure S1. Normalized UV-vis absorption spectra of FPt(OXD6TPA6Pic) in CH_2Cl_2 and PL spectra of PVK and PFO film at room temperature

Figure S2. Energy band diagram of FPt(OXD6TPA6Pic), PVK, PFO and PBD

Figure S3. EL spectra of devices B under different applied voltages at the dopant concentration of 8 wt%

Figure 1

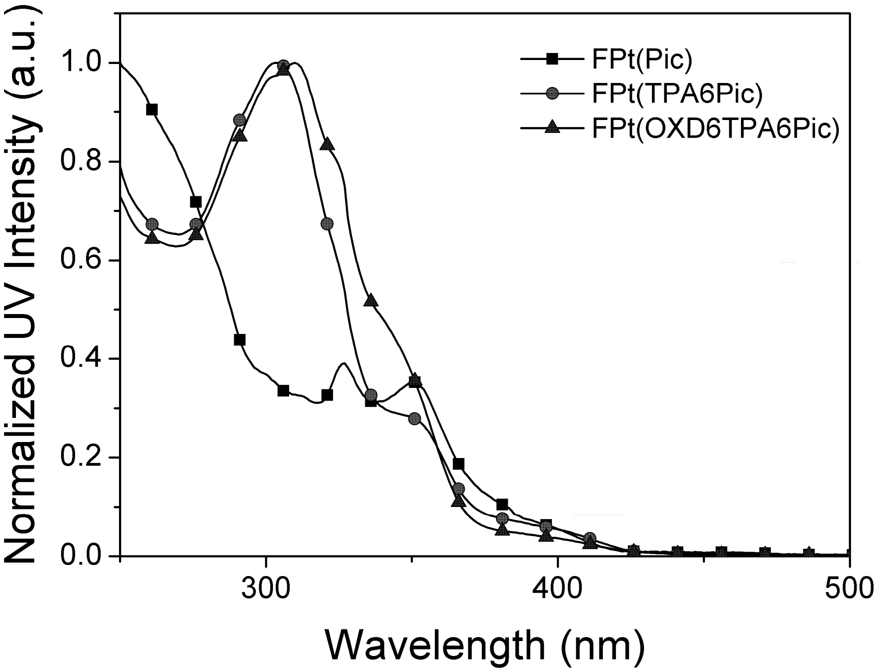
Normalized UV Intensity (a.u.)
0.0
0.2
0.4
0.6
0.8
1.0
300
400
500
Wavelength (nm)
FPt(Pic)
FPt(TPA6Pic)
FPt(OXD6TPA6Pic)

Figure 2

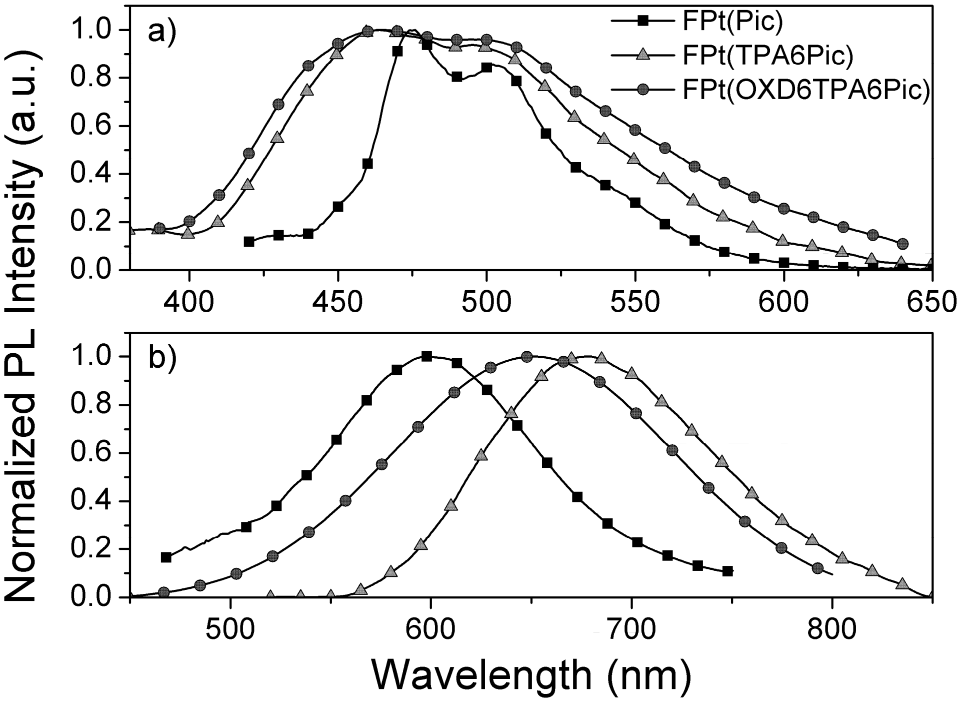
a)
b)
FPt(Pic)
FPt(TPA6Pic)
FPt(OXD6TPA6Pic)
Normalized PL Intensity (a.u.)
Wavelength (nm)
0.0
0.2
0.4
0.6
0.8
1.0
400
450
500
550
600
650
500
600
700
800

Figure 3

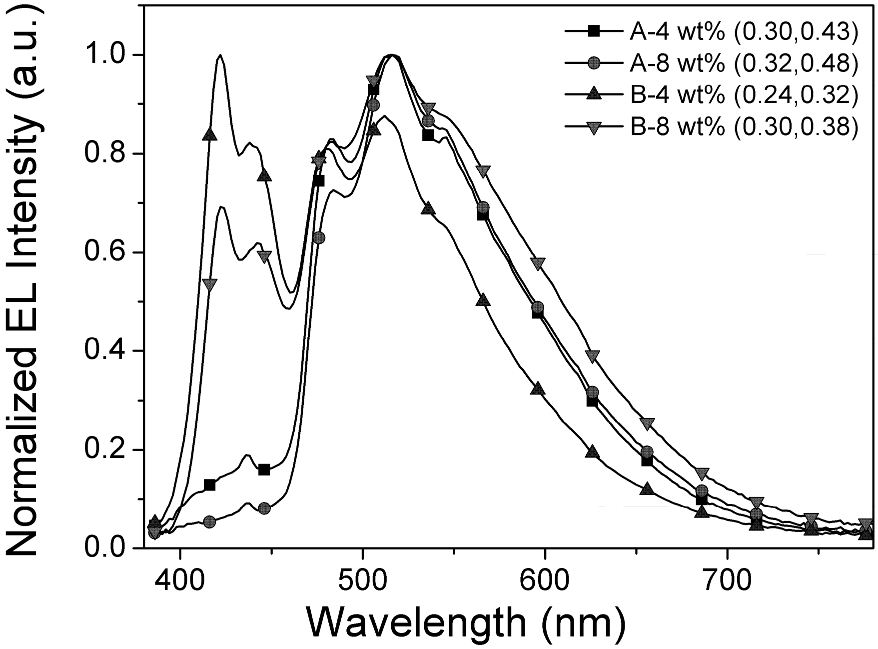
Normalized EL Intensity (a.u.)
Wavelength (nm)
0.0
0.2
0.4
0.6
0.8
1.0
400
500
600
700
A-4 wt% (0.30,0.43)
A-8 wt% (0.32,0.48)
B-4 wt% (0.24,0.32)
B-8 wt% (0.30,0.38)

Figure 4

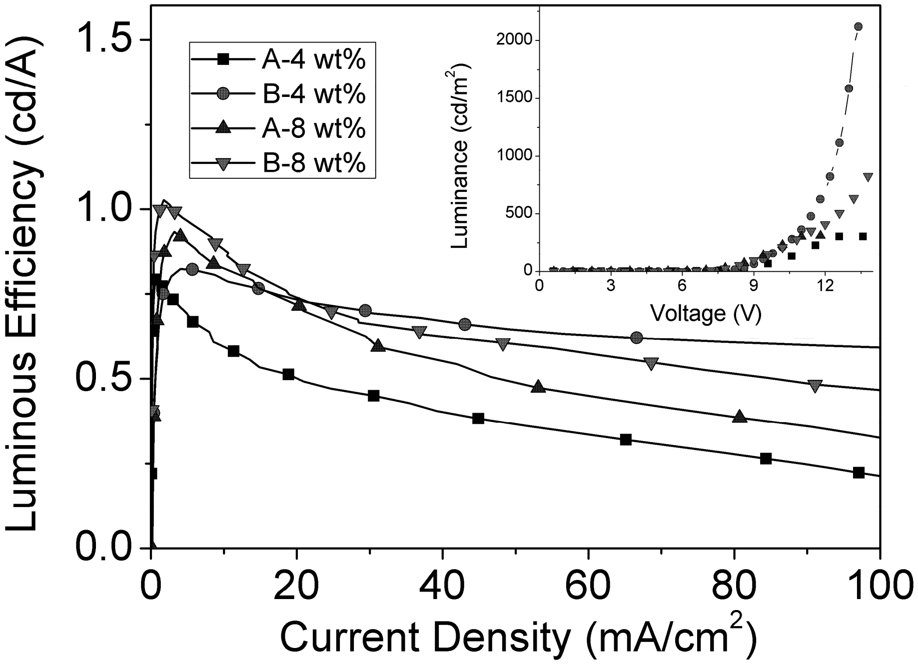
Luminous Efficiency (cd/A)
1.5
1.0
0.5
0.0
0
20
40
60
80
100
Current Density (mA/cm^2)
A-4 wt%
B-4 wt%
A-8 wt%
B-8 wt%
Luminance (cd/m^2)
2000
1500
1000
500
0
3
6
9
12
Voltage (V)

Scheme 1

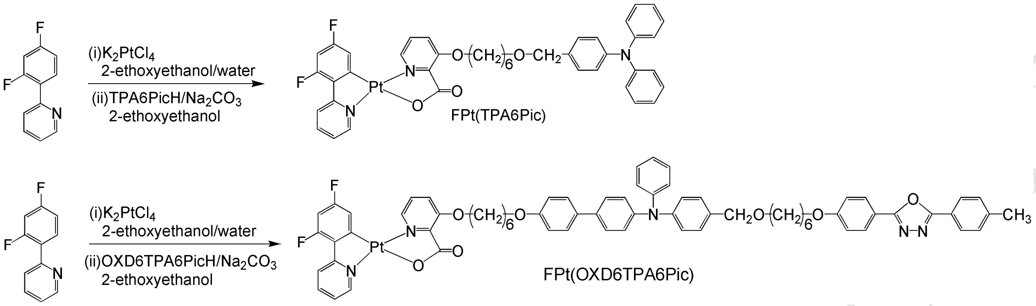
F
F
N
(i)K2PtCl4
2-ethoxyethanol/water
(ii)TPA6PicH/Na2CO3
2-ethoxyethanol
F
F
Pt
N
N
O
O
O
(CH2)6
O
CH2
N
FPt(TPA6Pic)
F
F
N
(i)K2PtCl4
2-ethoxyethanol/water
(ii)OXD6TPA6PicH/Na2CO3
2-ethoxyethanol
F
F
Pt
N
N
O
O
O
(CH2)6
O
N
CH2O
(CH2)6
O
O
N–N
CH3
FPt(OXD6TPA6Pic)

Figure S1

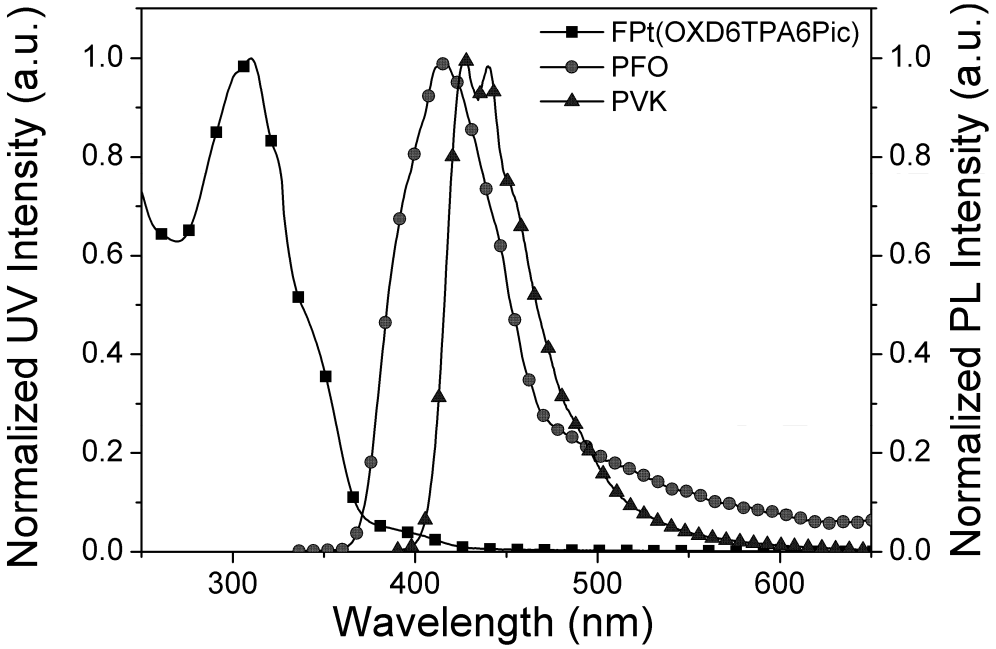
Normalized UV Intensity (a.u.)
Normalized PL Intensity (a.u.)
Wavelength (nm)
FPt(OXD6TPA6Pic)
PFO
PVK
0.0
0.2
0.4
0.6
0.8
1.0
300
400
500
600

Figure S2

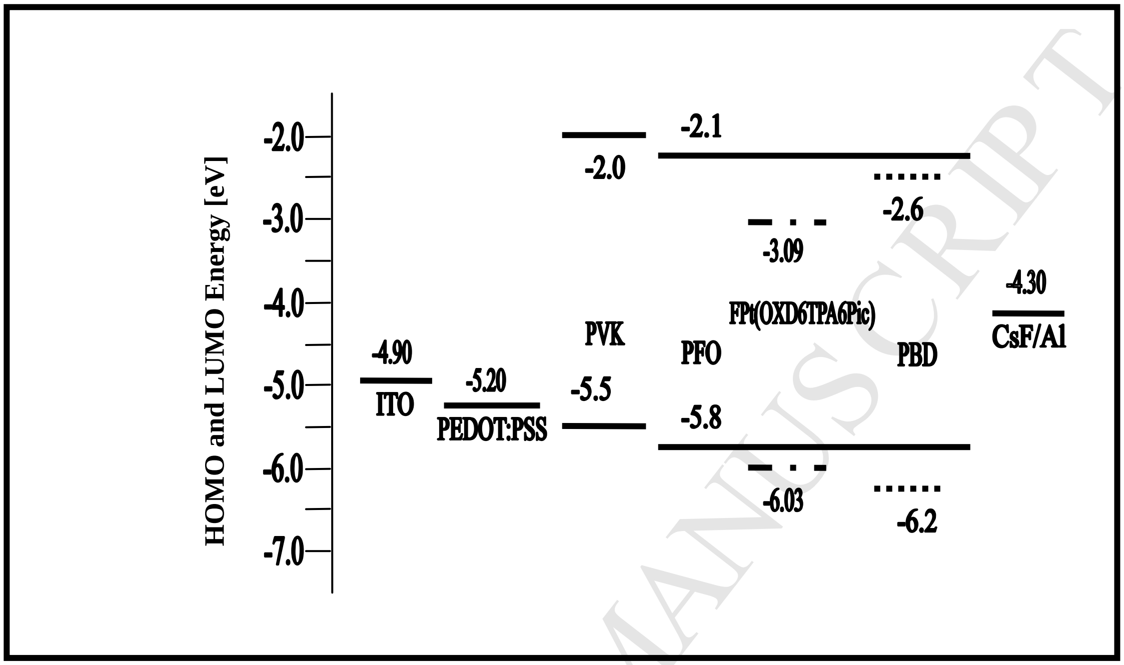
HOMO and LUMO Energy [eV]
-2.0
-3.0
-4.0
-5.0
-6.0
-7.0
-4.90
ITO
-5.20
PEDOT:PSS
-2.0
PVK
-5.5
-2.1
PFO
-5.8
-3.09
FPt(OXD6TPA6Pic)
-6.03
-2.6
PBD
-6.2
-4.30
CsF/Al

Figure S3

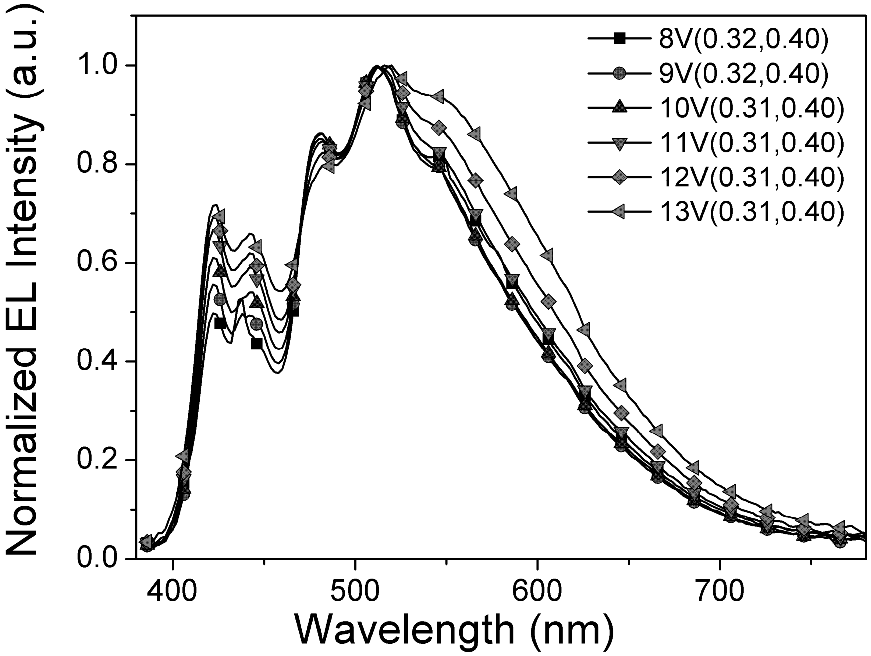
Normalized EL Intensity (a.u.)
0.0
0.2
0.4
0.6
0.8
1.0
400
500
600
700
Wavelength (nm)
8V(0.32,0.40)
9V(0.32,0.40)
10V(0.31,0.40)
11V(0.31,0.40)
12V(0.31,0.40)
13V(0.31,0.40)